

Workspace Analysis of 6–6 Cable-Suspended Parallel Robots

Arian Bahrami, Amir Teimourian

Abstract— In this paper, the effect of the moving platform size on the workspace volume of 6–6 cable-suspended parallel robots is investigated in details for different geometric configurations and orientations of the moving platform. The obtained hints can be used as a rule of thumb in designing this type of robot.

Keywords—Cable-suspended parallel robot, system analysis and design, workspace analysis.

I. INTRODUCTION

IN Cable Driven Parallel Robots (CDPRs), the moving platform is connected to the base platform by a number of cables. CDPRs have several advantages compared to traditional serial or parallel robots. They have high ratio of payload to robot weight and a much larger workspace which make them appropriate for high speed applications [1], lifting heavy loads [2], camera positioning in sports stadiums [3], service robot [4] and many others. Based on the number of cables (m) and the number of degrees of freedom (n), there are three categories for the CDPRs [5], [6], i.e. the incompletely restrained cable robots ($m < n+1$), the completely restrained cable robots ($m = n+1$) and the redundantly restrained cable robots ($m > n+1$). There have been some works in implementation of the incompletely restrained six cable robot such as NIST Robocrane [2] and the large scale FAST system [7].

The static equilibrium workspace of the cable robot is defined by the set of points where the mass center of the moving platform (MP) can be positioned while all the cables are in tension [8]. To this end, at each point within a search volume, the equation describing the force in each cable is used to check if tension is obtainable or not. Some authors attempted to tackle some aspects of the optimal design of incompletely restrained six cable robots by presenting the accuracy and workspace volume of the robot for several geometric configurations, various sizes and orientations of the base and the MPs [8]-[12].

In 2004, Pusey et al. [8] concluded that for any geometry of the base and MPs, the largest workspace volume occurs when the MP is the same size as the base platform (BP). In other words, for a fixed size of the BP, as the ratio of MP/BP increases, the workspace volume increases as shown in their Fig. 5.

In 2016, Bahrami and Nikkhah-Bahrami [11] pointed out that Pusey et al. [8] actually demonstrated the true effect of the BP size on the workspace volume instead of their mentioned intention to present the effect of the MP size. Although Pusey et al. [8] presented the true effect of the BP size on the workspace volume as mentioned by Bahrami and Nikkhah-Bahrami [11], to the best knowledge of the authors, there is still no work which presents the true effect of the MP size on the average workspace volume including non-zero orientations of a 6–6 cable-suspended parallel robot. Moreover, unlike prior works, the possible collision between a physical BP and MP is also considered in the present study. For these two major reasons, this work attempts to present the effect of the MP size on the average workspace volume of this type of cable robot while considering the possible collision between a physical BP and MP. The obtained hints and values are highly important in designing this type of cable robot and similar configurations.

II. KINEMATIC MODELING

The 6-6 cable-suspended parallel robot has a fixed platform, an MP and six cables each connected to a connection point on the MP A_i and one of the connection points on the fixed platform B_i , allowing six degrees of freedom as shown in Fig. 1. O_F is considered as the origin of the fixed frame XYZ which is located at the center of the BP and O_M is considered as the origin of the body frame xyz attached to the mass center of the MP. r_{base} is the radius distance from O_F to the connection points on the base platform B_i and r_{end} is the radius distance from O_M to the connection points on the moving platform A_i . Figs. 2 (a) and (b) show the γ angle of the BP (γ_{base}) and the MP (γ_{end}), respectively. The applied diagram of the model is shown in Fig. 3. This expression can be obtained from Fig. 3:

$$\mathbf{l}_i = \mathbf{p} + \mathbf{R}^M \mathbf{a}_i - \mathbf{b}_i, \quad i = 1, 2, 3, \dots, 6 \quad (1)$$

where \mathbf{b}_i is the position vector of the connection points on the base platform B_i in the fixed frame XYZ, ${}^M\mathbf{a}_i$ is the position vector of the connection points on the moving platform A_i in the body frame xyz, \mathbf{p} is the position vector of the point O_M , \mathbf{l}_i is the cable length vector from B_i to A_i , and \mathbf{R} is the rotation matrix of the MP with respect to the BP with three rotation angles ψ , θ , ϕ about the fixed axes of X, Y and Z, respectively which can be defined as:

Arian Bahrami and Amir Teimourian are with the Mechanical Engineering Department, Eastern Mediterranean University, G. Magosa, TRNC Mersin 10, Turkey (phone: +90 392 630 2598; e-mail: arian.bahrami@emu.edu.tr).

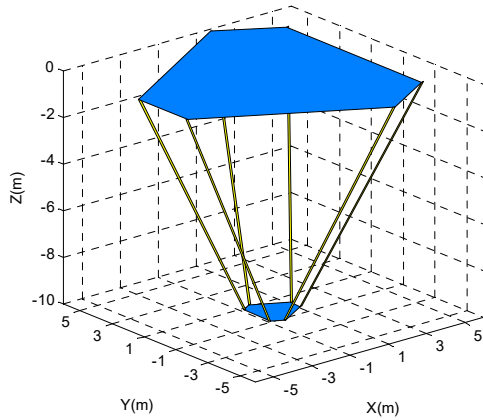
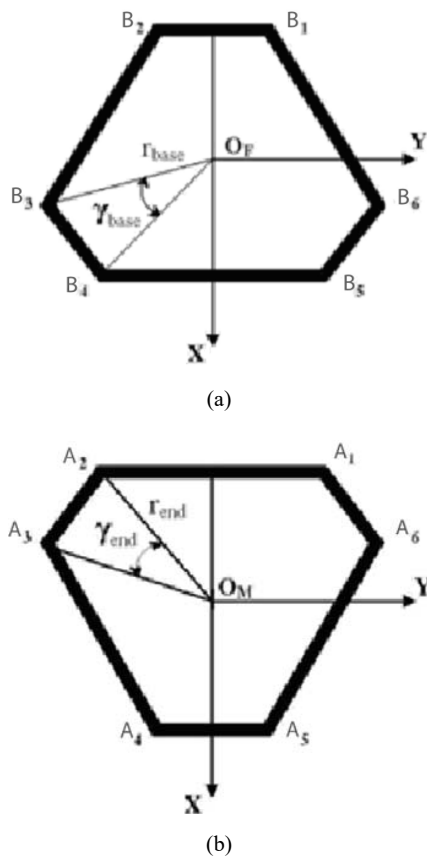


Fig. 1 The model of a 6-6 cable parallel robot


 Fig. 2 The γ angle for (a) the BP and (b) the MP

$$\mathbf{R} = \begin{bmatrix} \cos \phi \cos \theta & -\sin \phi \cos \psi + \cos \phi \sin \theta \sin \psi & \sin \phi \sin \psi + \cos \phi \sin \theta \cos \psi \\ \sin \phi \cos \theta & \cos \phi \cos \psi + \sin \phi \sin \theta \sin \psi & -\cos \phi \sin \psi + \sin \phi \sin \theta \cos \psi \\ -\sin \theta & \cos \theta \sin \psi & \cos \theta \cos \psi \end{bmatrix} \quad (2)$$

The cable length q_i can be defined as:

$$q_i = |\mathbf{l}_i| = (\mathbf{l}_i^T \mathbf{l}_i)^{1/2}, \quad i = 1, 2, 3, \dots, 6 \quad (3)$$

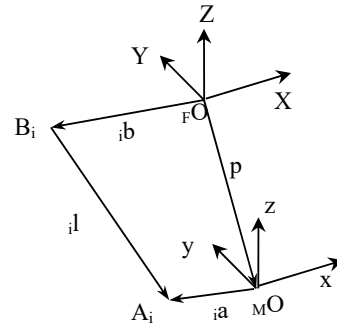


Fig. 3 The vector polygon diagram of the robot

The Jacobian matrix \mathbf{J} relates the twist of the MP $\mathbf{t} = [\mathbf{p}^T \quad \boldsymbol{\omega}^T]^T$ to the cable velocity vector $\dot{\mathbf{q}} = [\dot{q}_1 \quad \dot{q}_2 \quad \dot{q}_3 \quad \dot{q}_4 \quad \dot{q}_5 \quad \dot{q}_6]^T$, written as:

$$\dot{\mathbf{q}} = \mathbf{J} \mathbf{t} \quad (4)$$

where $\boldsymbol{\omega}^T$ is the angular velocity vector of the MP with respect to the fixed frame XYZ. The Jacobian matrix \mathbf{J} is represented such that its i th row is:

$$\mathbf{j}_i = \left[\left(\frac{\mathbf{l}_i}{|\mathbf{l}_i|} \right)^T \quad \left({}^B \mathbf{a}_i \times \frac{\mathbf{l}_i}{|\mathbf{l}_i|} \right)^T \right], \quad i = 1, 2, \dots, 6 \quad (5)$$

where,

$${}^B \mathbf{a}_i = \mathbf{R}^M \mathbf{a}_i \quad (6)$$

The relation between the cable tensions and external wrench on the MP can be defined as:

$$\mathbf{J}^T \mathbf{s} = \mathbf{F}_{\text{ext}} \quad (7)$$

where \mathbf{s} is the vector of cable tensions $\mathbf{s} = [s_1 \quad s_2 \quad s_3 \quad s_4 \quad s_5 \quad s_6]^T$, and \mathbf{F}_{ext} is the vector of external wrench applied to the MP, $\mathbf{F}_{\text{ext}} = [0 \quad 0 \quad -mg \quad 0 \quad 0 \quad 0]^T$. For calculating tension in the cables, (7) can also be written as:

$$\mathbf{s} = \mathbf{J}^{-T} \mathbf{F}_{\text{ext}} \quad (8)$$

The static equilibrium workspace is defined by the number of points where the mass center of the MP can be placed while all the cables must be in tension [8]. Therefore, at each point within the search volume if all the elements of the vector of the cable tensions obtained from (8) have nonnegative values $s_i \geq 0$, that point belongs to static equilibrium workspace volume.

III. RESULTS

A MATLAB program is created for analyzing the workspace volume of the 6-6 cable suspended robot which tests the points within the search space to define whether they belong to the static equilibrium workspace volume of the robot or not. The program input includes the size and the geometry of both platforms (r_{base} , r_{end} , γ_{base} , γ_{end}), the position and orientation of the MP, the desired search volume, and incremental step size for the search. To keep consistency, the values of the step size along all three axes, the search volume for possible workspace volume, and the geometry of both platforms are taken from Pusey et al. [8] as:

- The search volume is a cube with the dimensions: $-10 \leq Z \leq 0$ m, $-8 \leq Y \leq 8$ m, $-8 \leq X \leq 8$ m.
- The step size for the search is 0.4 m for all X, Y, and Z axes.
- The geometry of the BP is the same as the MP:

$$\gamma = \gamma_{base} = \gamma_{end}$$

By setting these values of the parameters and using (8), one can obtain the number of points as the workspace volume index.

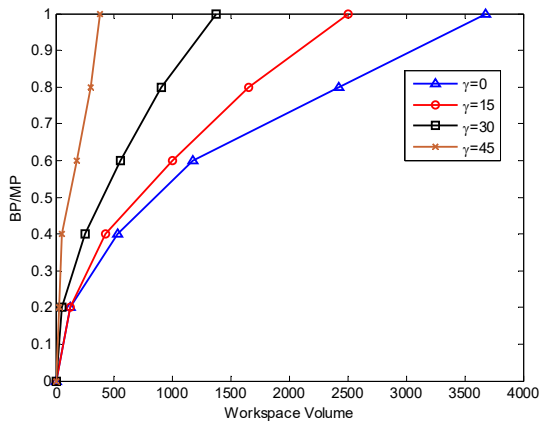


Fig. 4 The effect of the ratio of BP/MP on the workspace volume for orientation $\psi = \theta = \phi = 0$, $r_{end} = 6$ m

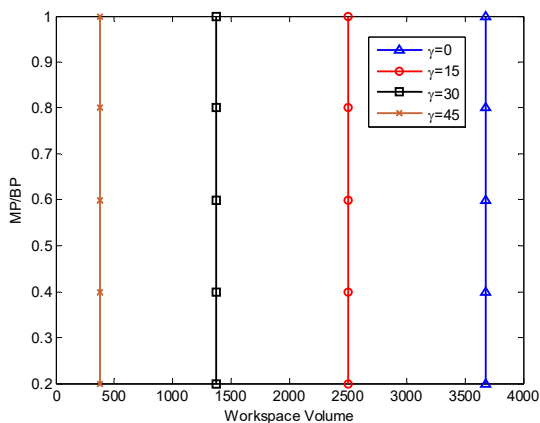


Fig. 5 The effect of the ratio of MP/BP on the workspace volume for orientation $\psi = \theta = \phi = 0$, $r_{base} = 6$ m

Fig. 4 demonstrates the variation of the workspace volume with respect to the ratio of BP/MP in case of zero rotation for different geometric configurations γ . It can be observed that for a fixed size of the MP, as the size of the BP increases, the workspace volume increases for all geometric configurations. Fig. 5 shows the effect of MP/BP on the workspace volume in case of zero rotation for different geometric configurations γ . It can be observed that for a fixed size of the BP, as the ratio of MP to BP changes, the workspace volume remains constant in case of zero rotation for all geometric configurations.

In attempting a broader range of studies besides the case of zero rotation $\psi = \theta = \phi = 0$, 637 different orientations are considered. The workspace volume is evaluated for all 637 constant orientation combinations of ψ, θ , and ϕ defined in Table I of [8] as:

- $-30 \leq \psi \leq 30, \Delta\psi = 10$
- $-30 \leq \theta \leq 30, \Delta\theta = 10$
- $-60 \leq \phi \leq 60, \Delta\phi = 10$

Due to the vast amount of information involved, the individual workspace volume shapes at every constant orientation are not presented. To reduce the amount of data pertaining to 637 orientations observed, averages of the workspace volume are used. All the obtained workspace volume values for 637 different roll, pitch and yaw angles are averaged for different geometric configurations, the BP and the MP sizes.

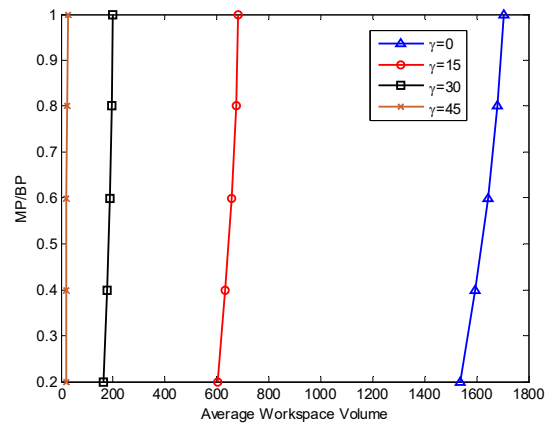


Fig. 6 The effect of the ratio of MP/BP on the average workspace volume ($r_{base} = 6$ m)

The variation of the average workspace volume is presented in Table I and Figs. 6 and 7. It is noticeable that the trend seen in Figs. 6 and 7 is nearly similar to the case of zero rotation presented in Figs. 4 and 5. The obvious difference is that when the size of the BP is constant, as the size of the MP increases, the average workspace volume increases.

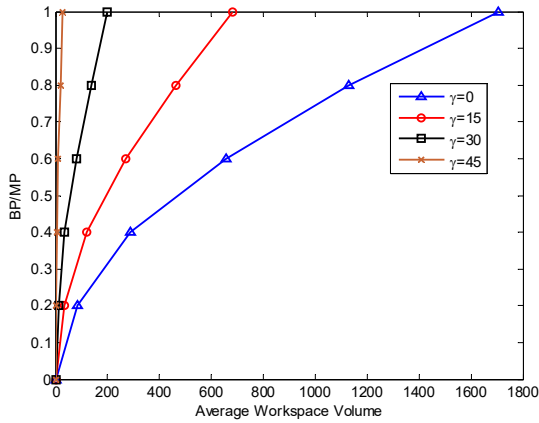


Fig. 7 The effect of the ratio of BP/MP on the average workspace volume ($r_{end}=6$ m)

TABLE I
AVERAGE WORKSPACE VOLUME WITHOUT THE EFFECT OF POSSIBLE COLLISION FOR DIFFERENT SIZES OF THE MP

MP/BP	$\gamma = 0$	15	30	45
0.2	1538.6	602.9	161.6	18.0
0.4	1595.5	633.3	176.0	18.3
0.6	1646.1	657.8	188.0	21.2
0.8	1681.3	674.7	196.0	24.4
1	1704.0	682.9	198.9	25.2

TABLE II
AVERAGE WORKSPACE VOLUME WITH THE EFFECT OF POSSIBLE COLLISION FOR DIFFERENT SIZES OF THE MP

MP/BP	$\gamma = 0$	15	30	45
0.2	1535.2	602.9	161.6	18.0
0.4	1578.6	633.0	176.0	18.2
0.6	1610.8	655.6	187.9	21.1
0.8	1615.5	666.9	195.2	24.3
1	1594.3	665.4	196.4	25.0
1.2	1551.7	650.2	193.4	25.4
1.4	1478.5	621.6	186.4	23.0
1.6	1404.7	588.4	173.9	19.5

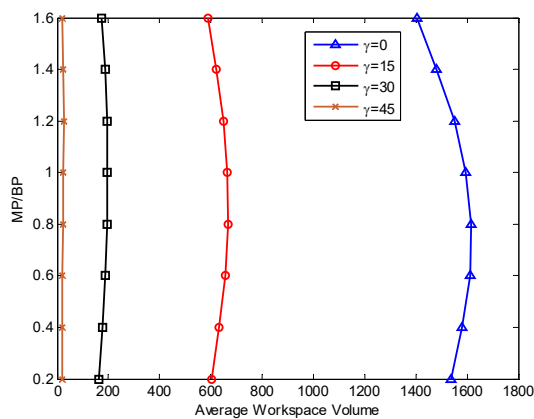


Fig. 8 Average workspace volume with the effect of possible collision for different sizes of the MP ($r_{base}=6$ m)

The average workspace volume difference between the smallest and largest sizes of the MP is about 10%, 13%, 23%, and 40% for the geometric configurations $\gamma = 0, 15, 30, 45$, respectively as presented in Table I. It should be mentioned that the possible collision between a physical BP and MP was not considered in [8] and our initial calculation. It is evident that as the size of the MP increases, the average workspace volume decreases due to an increase in the possibility of collision between two platforms for any small rotation of a larger MP near the BP. In other words, the average workspace volume difference would be less considering the possible collision which will be shown later in Fig. 8 and Table II.

Table II and Fig. 8 show the variation of the average workspace volume with respect to the size of the MP when the possible collision between a physical BP and MP is taken into account in the calculation. The z coordinate of all the MP vertices should be below the BP to avoid any possible collision formulated as:

$$\bar{\mathbf{k}} \cdot (\mathbf{p} + \mathbf{R}^M \mathbf{a}_i) < 0, \quad i = 1, 2, 3, \dots, 6 \quad (9)$$

It is noticeable from Fig. 8 that there exists an optimal MP size for any geometric configuration where the average workspace volume reaches its maximum value in this case. The average workspace volume reaches its maximum value at the MP/BP ratios of 0.73, 0.80, 0.93, and 1.20 for the geometric configurations $\gamma = 0, 15, 30, 45$, respectively. As a result, the optimal size of the MP increases with increasing the geometric configuration γ . Moreover, it can be deduced from Tables I and II that the effect of the possible collision on the average workspace volume is more significant for the geometric configuration $\gamma = 0$ while the effect is less significant for the geometric configuration $\gamma = 45$. These hints can be used as a rule of thumb in designing this type of robot and similar configurations.

IV. CONCLUSION

This paper presents the effect of the MP size on the workspace volume of 6–6 cable-suspended parallel robots considering different geometric configurations and orientations of the MP. The following conclusions were drawn:

- For a fixed size of the BP, as the ratio of MP/BP increases, the workspace volume remains constant for all geometric configurations in case of zero rotation of the MP.
- For a fixed size of the MP, as the ratio of BP/MP increases, the workspace volume increases for all geometric configurations in case of zero rotation of the MP.
- For a fixed size of the BP, as the ratio of MP/BP increases, the average workspace volume increases for all geometric configurations.
- The size of the MP has the least effect on the average workspace volume for the geometric configuration $\gamma = 0$

while it has the greatest effect on the average workspace volume for the geometric configuration $\gamma = 45^\circ$.

- There exists an optimal MP size for any geometric configuration where the average workspace volume reaches its maximum value when the effect of the possible collision between the BP and the MP is taken into account.
- The optimal size of the MP increases with increasing the geometric configuration γ .
- The effect of the possible collision on the average workspace volume is more significant for the geometric configuration $\gamma = 0^\circ$ while the effect is less significant for the geometric configuration $\gamma = 45^\circ$.

REFERENCES

- [1] S. Kawamura, W. Choe, S. Tanaka, and S. Pandian, "Development of an ultrahigh speed robot FALCON using wire drive system," in *Proc. IEEE/ICRA Int. Conf. Robot. Autom.* 1995, pp. 215–220.
- [2] J. Albus, R. Bostelman, and N. Dagalakis, "The NIST RoboCrane," *J. Robot. Syst.*, vol. 10, no. 5, pp. 709–724, 1992.
- [3] L. L. Cone, "Skycam: An aerial robotic camera system," *Byte*, vol. 10, no. 10, pp. 122–132, 1985.
- [4] S. Mustafa, G. Yang, S. Yeo, W. Lin, and I.M. Chen, "Self-calibration of a biologically inspired 7 DOF cable-driven robotic arm," *IEEE/ASME Trans. Mechatronics*, vol. 13, no. 1, pp. 66–75, 2008.
- [5] A. Ming, and T. Higuchi, "Study on multiple degree-of freedom positioning mechanism using wires (part 1)- concept, design and control," *Int. J. Jpn. Soc. Precision Eng.*, vol. 28, no. 2, pp. 131–138, 1994.
- [6] R. Verhoeven, "Analysis of the Workspace of Tendon-based Stewart Platforms," PhD thesis, University of Duisburg-Essen, 2004.
- [7] B. Duan, "A new design project of the line feed structure for large spherical radio telescope and its nonlinear dynamic analysis," *Mechatron.* vol. 9, no. 1, pp. 54–64, 1999.
- [8] J. Pusey, A. Fattah, S. Agrawal, E. Messina. "Design and workspace analysis of a 6-6 cable-suspended parallel robot," *Mech. Mach. Theory*, vol. 39, no. 7, pp. 761–778, 2004.
- [9] J. Hamed, A. Bahrami, M. Nikkhah-Bahrami, "Workspace sensitivity analysis of spatial cable robots," in *Proc IASTED Int. Conf. Robot, Robo* 2010, pp. 175–182.
- [10] A. Bahrami, M. Nikkhah-Bahrami, "Multi objective design of spatial cable robots," in *Proc 2nd IASTED Int. Conf. Robot, Robo* 2011, pp. 345–352.
- [11] A. Bahrami, M. Nikkhah-Bahrami. "Comments on "Design and workspace analysis of a 6-6 cable-suspended parallel robot"," *Mech. Mach. Theory*, vol. 98, pp. 1, 2016.
- [12] A. Bahrami, M. Nikkhah-Bahrami, "Optimal design of a spatial six-cable robot," in *Proc 2nd IASTED Int. Conf. Robot, Robo* 2011, pp. 134–141.